

# PHYSICAL REVIEW C

## NUCLEAR PHYSICS

THIRD SERIES, VOLUME 43, NUMBER 5

MAY 1991

### RAPID COMMUNICATIONS

*The Rapid Communications section is intended for the accelerated publication of important new results. Manuscripts submitted to this section are given priority in handling in the editorial office and in production. A Rapid Communication in Physical Review C may be no longer than five printed pages and must be accompanied by an abstract. Page proofs are sent to authors.*

#### Comparison of nucleus-nucleus interactions at 14.5–200A GeV with a multistring model

P. L. Jain, G. Singh, and K. Sengupta

*High Energy Experimental Laboratory, Department of Physics,  
State University of New York at Buffalo, Buffalo, New York 14260*

(Received 13 November 1990)

Multiplicity and angular distributions of shower, grey, and black particles produced in the interactions of  $^{32}\text{S}$  and  $^{16}\text{O}$  at 200A GeV, and  $^{16}\text{O}$  at 60A GeV, and  $^{28}\text{Si}$  at 14.5A GeV in emulsion are compared with the predictions of an event generator, which takes into account the intranuclear cascading. The data on shower and grey particles for all four beams are well described by the event generator. The black prong distributions show significant departure from the model.

The advent of heavy-ion beams at the CERN superproton synchrotron (SPS) and at the BNL alternating-gradient synchrotron (AGS) has opened a new field of ultrarelativistic heavy-ion collisions for systematic studies. In the past, data for many parameters of measurements have been compared with model predictions such as the Monte Carlo code FRITIOF,<sup>1</sup> but the experimental data have not been fitted in their entirety with this model. The main reason is that the cascade interactions, which play a very important role in nucleus-nucleus collisions, especially in the small rapidity region called the target fragmentation region, have not been incorporated properly in this model. Moreover, when the analysis is done at low incident energies (such as at BNL), the effect of the cascade interactions becomes all the more important. In order to fit the data with any good theoretical model, it should have the provision of cascading interactions. Thus, FRITIOF is not suitable at BNL energies. As far as we know, there has not been any previous successful attempt to fit the data of heavy-ion collisions both at CERN and BNL energies (with a difference of energy per nucleon by a factor of 20) of different projectile masses with just one theoretical model; this is the subject of this paper.

In this paper, we present the multiplicity distributions of shower particles ( $\beta > 0.7$ ) and their fluctuations in pseudorapidity intervals for  $^{32}\text{S}$  (beam A),  $^{16}\text{O}$  (beam B) at 200A GeV, and  $^{16}\text{O}$  (beam C) at 60A GeV from CERN SPS (Expt. No. EMU08),  $^{28}\text{Si}$  (beam D) at 14.5A

GeV from BNL AGS (Expt. No. 847), and also the multiplicity and angular distributions of the target-associated (slow) particles for all four beams. The experimental observations of different parameters are compared for all the beams (with different projectile masses), not only among themselves, but also with the theoretical predictions of the Monte Carlo code VENUS (Ref. 2) of the dual-parton model, which has intranuclear cascading incorporated in it. The parameter in VENUS (version 3.05) which determines rescattering is the *interaction radius*  $r_0$ . This means that whenever two particles come closer than  $r_0$ , they interact. It plays an important role in determining the energy density, and hence in the formation of quark gluon plasma.

In this experiment, stacks of Ilford G-5 and Fuji emulsions were exposed horizontally to beams A, B, and C at CERN, and to beam D at BNL. The primary interactions were found by along-the-track scanning of the emulsion plates for each of the projectiles A, B, C, and D, and are referred to as the *minimum-bias* events. From these samples, we have excluded the electromagnetic<sup>3</sup> and elastic-scattering events. Further details of the experiment, with comprehensive discussions of classification and identification of the events in emulsion, are given in Refs. 4 and 5. The emulsion detector is suitable for recording all charged particles and is particularly reliable for events with very high multiplicities of shower particles ( $\beta > 0.7$ ) with ionization  $I < 1.4I_0$  ( $I_0$  being the minimum ioniza-

TABLE I. The experimental average multiplicities of shower ( $\langle n_s \rangle$ ), black  $N_b$ , and grey  $N_g$  particles with the corresponding predictions of VENUS (given in parentheses).

Beam	Energy ( $A$ GeV)	$N_{ev}$ <sup>a</sup>	$r_0$ (fm)	$\sigma_{inel}$ (mg)	$\langle n_s \rangle$	$\langle N_b \rangle$	$\langle N_g \rangle$
<sup>32</sup> S	200	379	(0.5)	$1140 \pm 36$ (1208)	$79.20 \pm 4.1$ (80.10)	$4.97 \pm 0.26$ (0.46)	$2.25 \pm 0.12$ (2.08)
<sup>16</sup> O	200	345	(0.5)	$1101 \pm 60$ (1039)	$57.30 \pm 3.1$ (57.77)	$5.39 \pm 0.29$ (0.49)	$2.03 \pm 0.11$ (1.97)
<sup>16</sup> O	60	282	(0.9)	$990 \pm 44$ (1015)	$34.12 \pm 2.3$ (36.32)	$4.91 \pm 0.34$ (0.78)	$2.16 \pm 0.15$ (2.64)
<sup>28</sup> Si	14.5	396	(1.35)	$1010 \pm 36$ (1204)	$30.75 \pm 1.5$ (28.78)	$6.86 \pm 0.34$ (1.43)	$2.91 \pm 0.15$ (2.95)

<sup>a</sup> $N_{ev}$  denotes number of events.

tion) in the very forward direction, grey particles with  $0.2 < \beta < 0.7$  or  $1.4I_0 < I < 5.0I_0$  (remnants of intranuclear cascade), and black particles with  $\beta < 0.2$  or  $I > 5I_0$  (evaporation prongs with very short track lengths) produced in ultrarelativistic heavy-ion collisions in a  $4\pi$  geometry. The angles of the shower tracks in the forward direction are measured with an accuracy of better than 0.1 mrad.<sup>5</sup>

The data samples used here are given in Table I. The normalized pseudorapidity ( $\eta_{lab}$ ) distributions of charged shower particles for beams  $A$ ,  $B$ ,  $C$ , and  $D$  are shown in Figs. 1(a)–1(d), respectively. The experimental data are compared with 1000 minimum-bias events generated for each of the beams  $A$ ,  $B$ ,  $C$ , and  $D$  using the Monte Carlo code VENUS, which stored the stable charged particles only. The fraction of the events from the different target nuclei in emulsion was generated using the known chemical composition of emulsion as an input to the model. The inelastic cross sections  $\sigma_{inel}$  of the simulated events and the average multiplicities ( $\langle n_s \rangle$ ) are in good agreement with the data for all the beams, as shown in Table I. The shapes of the experimental pseudorapidity distributions

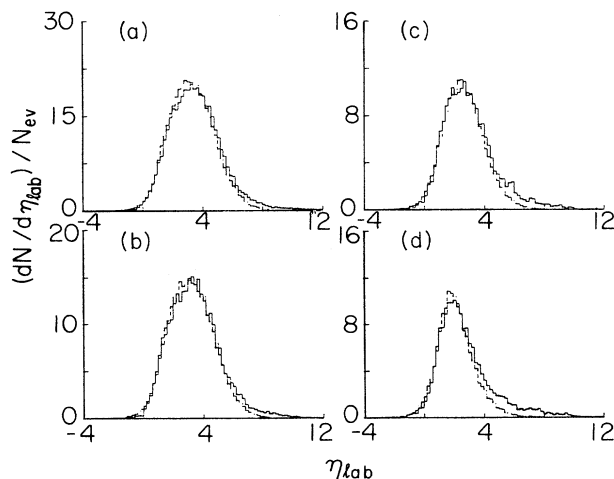


FIG. 1. The normalized pseudorapidity distributions for (a) 200A GeV <sup>32</sup>S, (b) 200A GeV <sup>16</sup>O, (c) 60A GeV <sup>16</sup>O, and (d) 14.5A GeV <sup>28</sup>Si. The broken histograms are the corresponding predictions of VENUS.

are reproduced quite well in each of the beams, except in the very forward region, where the spectator fragments of the projectile play an important role and for which the VENUS model has no provision. In order to compare the relative widths and heights of the  $\eta_{lab}$  distributions, the pseudorapidity distributions for all the four beams are shown in Fig. 2(a). The heights and widths of the  $\eta_{lab}$  distributions increase with the increase in the energy and mass of the projectile. The peak values of  $\eta_{lab}$  distributions for beams  $A$  and  $B$  lie near  $\eta_{lab} \approx 3.4$ , and for beams  $C$  and  $D$  near  $\eta_{lab} \approx 2.4$  and 2, respectively. Beam  $D$  has a long tail due to projectile fragmentation and also the peak value of its  $\eta_{lab}$  distribution for shower particles has

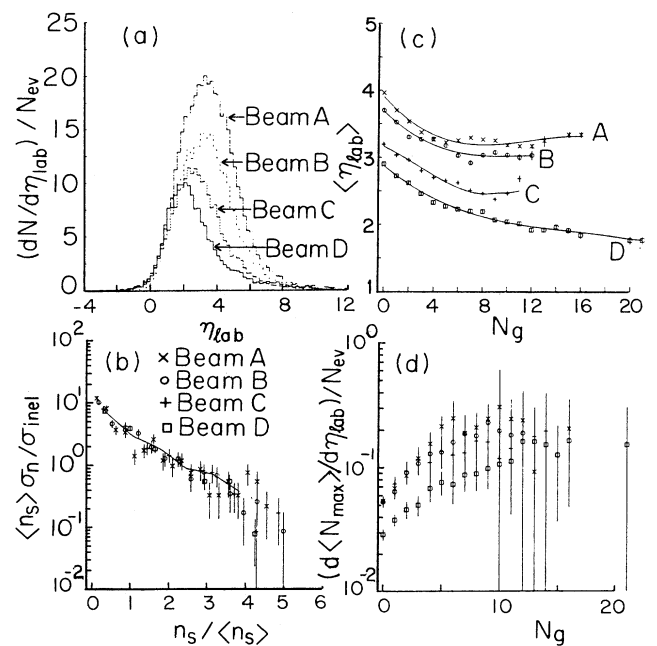


FIG. 2. (a) A comparison of the pseudorapidity distributions corresponding to the four projectiles. (b)  $\langle n_s \rangle \sigma_n / \sigma_{inel}$  as a function of  $n_s / \langle n_s \rangle$ : 200A GeV <sup>32</sup>S ( $\times$ ), 200A GeV <sup>16</sup>O ( $\circ$ ), 60A GeV <sup>16</sup>O ( $+$ ), and 14.5A GeV <sup>28</sup>Si ( $\square$ ). The solid curve is the prediction of VENUS pertaining to the <sup>28</sup>Si projectile. (c)  $\langle \eta_{lab} \rangle$  as a function of  $N_g$ . The curves represent polynomial fits to the data. (d)  $(d\langle N_{max} \rangle / d\eta_{lab}) / N_{ev}$  as a function of  $N_g$ .

the lowest value in comparison to the other beams. The part of the distribution for  $\eta_{\text{lab}} \leq 1.8$  (target fragmentation region) for all the beams remains unchanged, which is due to the phenomenon of limiting fragmentation.<sup>5</sup> The multiplicity distribution of shower particles ( $n_s$ ) for each beam, just like the  $\eta_{\text{lab}}$  distribution, is well reproduced by VENUS. This leads us to compare the multiplicity distributions  $\langle n_s \rangle \sigma_n / \sigma_{\text{inel}}$  in the normalized form  $n_s / \langle n_s \rangle$  for all four beams. These exhibit a universal scaling irrespective of the projectile mass and energy and are shown in Fig. 2(b). Here,  $\sigma_n$  and  $\sigma_{\text{inel}}$  are the partial and total cross sections, respectively. The theoretical predictions due to the model VENUS for respective beams fit the data in Fig. 2(b) quite well. For the sake of clarity we show here the theoretical predictions for the  $^{28}\text{Si}$  beam *D* only. The origin of the multiplicity scaling in minimum-bias events is a consequence of the nuclear geometry and reflects the distribution of the participating nucleons from the two interacting nuclei.

The violence of the nuclear collision is generally measured by the transverse energy, which is related to the number of (intranuclear) collisions ( $\nu$ ). They ( $\nu$ ) are further correlated nonlinearly with the observed number of grey tracks  $N_g$  (Ref. 6) which are mostly recoil protons with a kinetic energy of  $20 < T < 375$  MeV. The linear increase in the  $\langle n_s \rangle$  vs  $N_g$  depends on the projectile mass as well as on its energy. This is exhibited through the increase in its slope.<sup>7</sup> We now discuss how the energy of the projectile is distributed among the secondary shower (cascading) particles, as observed by the production of  $N_g$ . A strong correlation between the excitation energy observed through the production of grey particles ( $N_g$ ) and the charged particle multiplicity ( $n_s$ ) is emphasized by the behavior of  $\langle \eta_{\text{lab}} \rangle$  as a function of  $N_g$ . We present the characteristics of  $\langle \eta_{\text{lab}} \rangle$  distributions in Fig. 2(c), which decrease monotonically with  $N_g$  for all four beams (where the data points have been fitted with polynomials). The distributions at any  $N_g$  conserve approximately the constant difference  $\langle \eta_{\text{lab}} \rangle_i - \langle \eta_{\text{lab}} \rangle_j$  for any two beams *ij*. All curves slowly decrease due to the loss of the projectile energy which has to be shared by more and more particles at less and less  $\eta_{\text{lab}}$  or energy with the increasing number of collisions (large  $N_g$ ); eventually these curves level off. The loss (slopes) of  $\langle \Delta \eta_{\text{lab}} \rangle$  is the first few values of  $N_g$  is more in the heavier beam *A* as compared to beam *B* at the same energy per nucleon, and is followed by beams *C* and *D*. In beam *D*, the distribution  $\langle \eta_{\text{lab}} \rangle$  continues decreasing for large values of  $N_g$ , and its loss ( $\langle \eta_{\text{lab}} \rangle_{\text{max}} - \langle \eta_{\text{lab}} \rangle_{\text{plateau}}$ ), as compared to other beams, is over the whole  $\eta_{\text{lab}}$  range. It is almost double that of any other beam (*A*, *B*, or *C*) and has the maximum energy loss with respect to its primary energy. Hence, we observe the largest amount of nuclear stopping for beam *D*. Plotted in Fig. 2(d) is the normalized distribution of  $(d\langle N_{\text{man}} \rangle / d\eta_{\text{lab}}) / N_g$  vs  $N_g$  for all four beams. For beams *A*, *B*, and *C*, we find that the distributions are independent of the projectile masses and energies. This shows a limiting behavior of the minimum-bias samples for beams *A*, *B*, and *C* at any value of  $N_g$ , i.e., the events corresponding to a fixed impact parameter in terms of geometrical models. However, when we use a projectile of much less energy, i.e.,  $^{28}\text{Si}$  at 14.5A GeV

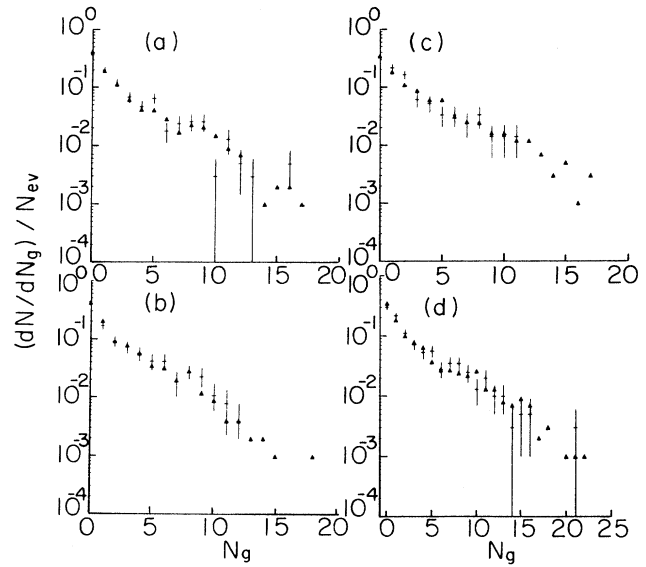


FIG. 3. The normalized multiplicity distributions of grey prongs for (a) 200A GeV  $^{32}\text{S}$ , (b) 200A GeV  $^{16}\text{O}$ , (c) 60A GeV  $^{16}\text{O}$ , and (d) 14.5A  $^{28}\text{Si}$ . The corresponding VENUS predictions ( $\blacktriangle$ ) are shown in each case.

(beam *D*), the distribution as shown in Fig. 2(d) has approximately the same shape as shown for other beams (*A*, *B*, and *C*) together, but the magnitude of the density per  $N_g$  for beam *D* is reduced to almost half the values of beams *A*, *B*, and *C*.

The normalized multiplicity distributions of grey ( $N_g$ ) particles for four beams are compared with reference samples generated by VENUS in Fig. 3. The agreement is very

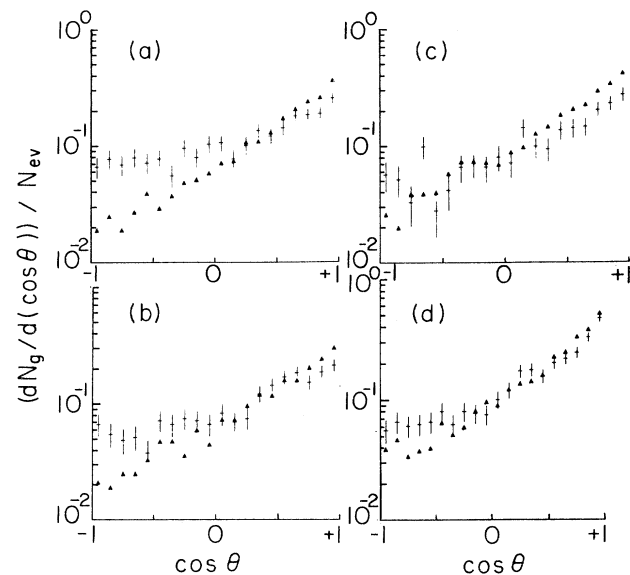


FIG. 4. The normalized angular distributions of grey prongs at (a) 200A GeV  $^{32}\text{S}$ , (b) 200A GeV  $^{16}\text{O}$ , (c) 60A GeV  $^{16}\text{O}$ , and (d) 14.5A GeV  $^{28}\text{Si}$ . The corresponding VENUS predictions ( $\blacktriangle$ ) are shown in each case.

good for the values of  $r_0$  indicated in Table I. Beam *D* has the longest tail for large values of  $N_g$ , as is also shown in Fig. 2(c). Figure 4 exhibits the angular distribution of grey particles for projectiles *A*, *B*, *C*, and *D*, along the corresponding predictions from VENUS. The distributions in Fig. 4 are distinctly anisotropic for recoil particles emerging from interactions of the projectiles considered. In general, the model reproduces the shapes of the angular distributions of grey particles from all beams quite well, except in the region of  $\cos\theta < -0.3$ , and the best results are obtained for beam *D* [Fig. 4(c)].

The experimental results for shower particles ( $n_s$ ) and grey particles ( $N_g$ ) are well reproduced by VENUS. The multiplicity distributions for black prongs ( $N_b$ ) for the four beams are shown in Fig. 5, while the same distributions obtained from VENUS show significant departure from the data for the same set of values of  $r_0$  used in the context of the  $N_g$  distributions. The failure of VENUS to describe the multiplicity distribution of black prongs (target protons) is a natural consequence of the simple geometry described by the Monte Carlo code. Theoretical predictions from VENUS for beams *A*, *B*, and *C* are far away from the corresponding data points, while for beam *D* they are relatively closer to the experimental observations. For  $r_0$  values different from those given in Table I, the theoretical values are less than those shown in Fig. 5. The kinks in the experimental distributions at  $N_b \approx 8$  may be due to the change of impact parameter from collisions with light (C, N, O) to heavy (Ag, Br) targets in emulsion.

The multiplicity and angular distributions of shower ( $n_s$ ) and grey ( $N_g$ ) particles are successfully reproduced by the theoretical multistring model VENUS at CERN and BNL energies. However, the simple rescattering mechanism included in VENUS is inadequate for explaining the distribution of the black particles. It needs a full intranu-

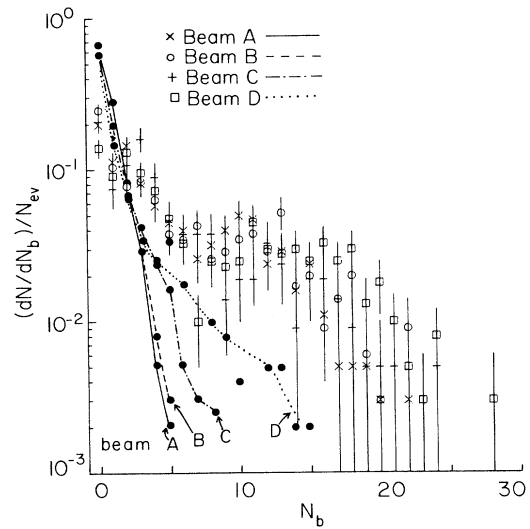


FIG. 5. A comparison of the multiplicity distributions of black prongs corresponding to the four projectiles. The VENUS predictions ( $\bullet$ ) are shown for each of these incident beams by hand-drawn lines.

clear cascade which includes all subsequent collisions of hadrons created in the secondary collisions.

We are thankful to the technical staff and the emulsion operating group of CERN and BNL for their help in the exposures. We appreciate the help from Professor G. Romano and Dr. H. Sletten, Dr. J. Wotschach, Dr. D. Beavis, and Dr. M. Kazuno. We also thank Dr. K. Werner for providing us with the model VENUS. This work was supported by the Department of Energy under Grant No. DE-FGO2-90ER40566.

<sup>1</sup>B. Andersson *et al.*, Phys. Rep. **97**, 31 (1983).

<sup>2</sup>K. Werner, Phys. Lett. B **208**, 520 (1988); Phys. Rev. D **39**, 780 (1989).

<sup>3</sup>G. Singh, K. Sengupta, and P. L. Jain, Phys. Rev. C **4**, 999 (1990).

<sup>4</sup>G. Singh, K. Sengupta, and P. L. Jain, Phys. Rev. Lett. **61**, 1073 (1988); K. Sengupta, G. Singh, and P. L. Jain, Phys. Lett. B **213**, 548 (1988).

<sup>5</sup>P. L. Jain, K. Sengupta, G. Singh, and A. Z. M. Ismail, Phys. Lett. B **235**, 351 (1990); K. Sengupta, G. Singh, and P. L. Jain, Mod. Phys. Lett. A **5**, 285 (1990); P. L. Jain, R. D.

Malucci, and M. J. Potoczak, Phys. Rev. Lett. **24**, 526 (1970); M. I. Adamovich *et al.*, Phys. Rev. Lett. **62**, 2801 (1989).

<sup>6</sup>M. K. Hegab and J. Hufner, Phys. Lett. **105B**, 103 (1981); M. K. Hegab and J. Hufner, Nucl. Phys. A **384**, 353 (1981); W. Q. Chao, M. K. Hegab, and J. Hufner, Nucl. Phys. A **395**, 482 (1983); B. Andersson, I. Otterlund, and E. Stenlund, Phys. Lett. **73B**, 343 (1978); P. L. Jain, K. Sengupta, and G. Singh, Nuovo Cimento A **99**, 9 (1988).

<sup>7</sup>P. L. Jain, K. Sengupta, and G. Singh, Phys. Rev. C (submitted).